Doi: 10.1111/j.1742-7843.2009.00472.x
Journal compilation © 2009 Nordic Pharmacological Society. *Basic & Clinical Pharmacology & Toxicology*, **106**, 53–61

Effects of Insulin-Like Growth Factor-1 on Rotenone-Induced Apoptosis in Human Lymphocyte Cells

Isabel Cristina Avila-Gomez, Carlos Velez-Pardo and MarleneJimenez-Del-Rio

School of Medicine, Medical Research Institute, Neuroscience Research Program, University of Antioquia, Medellin, Colombia

(Received 17 March 2009; Accepted 4 August 2009)

Abstract: Human peripheral blood lymphocytes have been useful as a putative model of oxidative stress-induced apoptosis for Parkinson's disease. The present work shows that rotenone, a mitochondrial complex I inhibitor, induced time- and concentration-dependent apoptosis in lymphocytes which was mediated by anion superoxide radicals ($O_2\bullet^-$)/hydrogen peroxide, depolarization of mitochondria, caspase-3 activation, concomitantly with the nuclear translocation of transcription factors such as NF-κB, p53, c-Jun and nuclei fragmentation. Since insulin-like growth factor-1 (IGF-1) interferes with a cell's apoptotic machinery when subjected to several stressful conditions, it is demonstrated here for the first time that IGF-1 effectively protects lymphocytes against rotenone through PI-3K/Akt activation, down-regulation of p53 and maintenance of mitochondrial membrane potential independently of ROS generation. These data might contribute to understanding the role played by IGF-1 against oxidative stress stimuli.

Parkinson's disease is a neurodegenerative disorder characterized by progressive degeneration of dopaminergic neurons in the *substantia nigra* pars compacta. Unfortunately, despite several decades of investigation in Parkinson's disease, neuroprotection remains the most important unmet need of this disorder. It has thus become crucial to investigate innovative pharmacotherapy approaches aimed at slowing or reducing the progress of neuronal loss in Parkinson's disease. However, the cell death molecular machinery involved in causal dysfunction and dopaminergic neuron demise must be unravelled to fully attain this objective. Although the exact cause of dopaminergic cell deterioration in Parkinson's disease remains unknown, dysfunction of mitochondria [1], genetic factors [2] and environmental exposure to neurotoxins, or a combination of them [3] have all been suggested as being the basis of Parkinson's disease cases.

Epidemiological studies have indicated that pesticides may be a risk factor for Parkinson's disease [4]; it is thus interesting that rotenone, a naturally occurring insecticide, piscicide and pesticide isolated from plant species belonging to the *Derris* and *Lonchorcarpus* genera, is widely used for modelling Parkinson's disease [5]. One potential mechanism by which rotenone may cause dopaminergic loss is through disruption of mitochondrial function [6] and apoptosis, a type of programmed cell death. Indeed, this xenobiotic compound irreversibly binds to NADH dehydrogenase complex (also known as complex I) of the mitochondrial electron transport chain, thereby allowing the reduction of molecular oxygen (O_2) to superoxide radical ($O_2\bullet^-$) by the N2 iron sulphur cluster [7]. However, whether complex I impairment causes dopaminergic neurodegeneration via oxidative stress or through bioenergetic defects remains controversial [8, 9 *versus* 10, 11].

Likewise, some investigators have reported that rotenone activates the caspase-3 executor protein in ventral mesencephalic dopaminergic neurons [11,12] and HL-60 (human promyolocyte leukaemia cell line) [13,14] and induces activation of the stress response c-Jun N-terminal protein kinase pathway in human neuroblastoma SH-SY5Y cells as a common toxin-mediated mechanism of dopaminergic cell apoptosis [15]. Other authors have found that rotenone induces neither c-Jun N-terminal protein kinase nor caspase-3 activation in human neuroblastoma SK-N-MC-cells or pheochromocytoma PC12 cells [16,17]. Moreover, rotenone may [18] or may not [15] promote cell death in PC12 cells. Therefore, the complete molecular mechanism of rotenone-induced cell death has not yet been fully established in a single cell model.

At present, a vast amount of evidence suggests that neurotrophic factors play a major role in neurodegenerative diseases, including Parkinson's disease. Insulin-like growth factor-I (IGF-1) has particularly been demonstrated to interfere with a cell's apoptotic machinery [19,20]. This feature makes IGF-1 an interesting molecule in understanding survival signals against stressful conditions [21] and a rational therapeutic candidate in neuroprotection strategies in Parkinson's disease [22]. Lymphocytes thus appear to be particularly fascinating non-neural cells for modelling dopaminergic cell death for at least three main reasons. First, lymphocytes and neurons are post-mitotic cells (i.e. they become locked in

Author for correspondence: Marlene Jimenez-Del-Rio, School of Medicine, Medical Research Institute, Neuroscience Research Program, University of Antioquia (UdeA), Calle 62 # 52-59, Building 1, Room 412; SIU-Medellin, Colombia (fax +574 219 64 44, e-mail marlene.jimenez@neurociencias.udea.edu.co).

the G_0 phase of the cell cycle). This feature causes molecules active in non-mitotic and mitotic cell division (e.g. NF-κB [23]) to be exclusively expressed in G_0, thus avoiding misleading interpretation in cause-effect experiments. Second, lymphocytes express the catecholaminergic system, including tyrosine hydroxylase (TH), monoamine oxidase [24 and references within], dopamine transporter [25] and dopamine D2-, D3-, D4- and D5-like receptors [26–30]. Third, both kinds of cells express similar molecular death machinery leading to the typical morphological and biochemical characteristics of apoptosis [31,32]. Given that lymphocytes express IGF-1 receptors [33,34], the present investigation was aimed at disentangling rotenone-induced death-signalling in lymphocytes and the survival molecular signalling downstream of IGF-1R as a response to rotenone-mediated toxic stimuli.

Materials and Methods

Materials. Reagents were purchased from Sigma-Aldrich (St. Louis, MO, USA) if not otherwise specified and were of analytical grade or better. 3,3′-dihexyloxacarbocyanine iodide ($D_iOc_6(3)$, Cat. #D-273) and dihydrorhodamine (cat. #D-633) were obtained from Invitrogen Molecular Probes (Eugene, OR, USA). The caspase-3 inhibitor (Ac–Ala–Ala–Val–Ala–Leu–Leu–Pro–Ala–Val–Leu–Leu–Ala–Leu–Leu–Ala–Pro–Asp–Glu–Val–Asp–CHO; DEVD, Cat # 260-046-M001) was from Alexis Biochemical Corporation (San Diego, CA, USA). Ammonium pyrrolidinedithiocarbamate (PDTC, cat. # 548000) and 1,9-pyrazoloanthrone (SP600125, cat # 420119) were acquired from Calbiochem (San Diego, CA, USA).

Isolation of lymphocytes. Peripheral blood lymphocytes were obtained from healthy adult (30–40 years old) males' venous blood by gradient centrifugation (lymphocyte separation medium, density: 1.007 G/M; Bio-Whittaker Inc., Walkersville, MD, USA). Isolated peripheral blood lymphocytes were washed three times with phosphate-buffered saline (10 mM sodium phosphate, 160 mM NaCl, pH 7.4) and suspended in RPMI 1640 (GIBCO laboratories, Grand Island, NY, USA) plus 10% foetal calf serum (FCS, GIBCO laboratories). This purification procedure gave >95% lymphocytes as determined by flow cytometry staining for $CD3^+$, $CD19^+$, $CD20^+$ and $CD19^+/20^+$ antigens. Peripheral blood lymphocytes in suspension were cultured in RPMI1640 supplemented with 10% foetal calf serum, 2 mM L-glutamine, 100 U/ml penicillin and 100 mg/ml streptomycin and then plated in 24 wells (1×10^6 cells/ml/well).

Experiments with peripheral blood lymphocytes. Morphological assessment of cell death by fluorescence microscopy using AO/EB double staining. The cell suspension (1 ml, final volume) was exposed to increasing rotenone concentration (1, 10, 100, 250 μM rotenone) freshly prepared in RPMI-1640 medium in the absence or presence of IGF-1 (250 nM) and different products of interest for 24 hr. at 37/C. The peripheral blood lymphocytes were then used for fluorescent microscopy analysis. After treatment, cells were mixed with 1 μl acridine orange (100 μg/ml AO final concentration) and ethidium bromide (100 μg/ml EB final concentration); 5 μl were placed on a slide and examined by fluorescence microscope (Zeiss Axiostart 50; Zeiss Wöhlk-Contact-Linsen, Gmb Schönkirchen, Germany). Normal peripheral blood lymphocytes cells (bright green chromatin) could be discriminated from early apoptotic cells (bright green highly condensed or fragmented chromatin), late apoptotic cells (bright orange highly condensed or fragmented chromatin) and necrotic cells (bright orange/red chromatin) based on AO/EB fluorescent DNA binding dye differential uptake. Apoptotic morphology was quantified by counting a minimum of 300 total cells as follows: % apoptotic cells = 100 × (total number of early and late apoptotic cells/total number of cells). Necrotic cells were not detected in the present experimental conditions. The apoptotic indexes were assessed three times in independent experiments.

Evaluation of intracellular reactive oxygen species. Assessment of superoxide anion radical generation. Superoxide anion radicals were evaluated as described elsewhere [35]. Briefly, lymphocytes (1 ml, final volume) were exposed to increasing rotenone concentrations in the same experimental conditions as mentioned above (at 0, 1, 3, 6, 12 and 24 hr.). The cells were then incubated with nitroblue tetrazolium (1 mM final concentration) for 1 hr. Nitroblue tetrazolium is an electrophilic dicationic compound which can easily accept electrons from electron donors (e.g. $O_2\bullet^-$). Nitroblue tetrazolium chloride is a yellow compound soluble in aqueous medium in its oxidized form. Its reduction to formazan is accompanied by the disappearance of positive charges resulting in a substantial decrease in solubility and the appearance of an intense blue-purple precipitate. The cells were examined for formazan formation after their incubation; formazan was quantified by counting a minimum of 300 total cells as follows: % formazan positive cells = 100 × (total number of blue cells / total number of cells). The assessment was repeated three times in independent experiments.

Assessment of hydrogen peroxide. Hydrogen peroxide (H_2O_2) can be detected in cell systems by using sensitive, uncharged, non-fluorescent dihydrorhodamine 123, as described elsewhere [36]. Briefly, peripheral blood lymphocytes (1×10^6 cells/ml) were incubated with increasing concentrations of rotenone (1–250 μM) and other products of interest. 100 μl untreated and treated peripheral blood lymphocyte aliquots were incubated in the presence of 10 nM dihydrorhodamine (20 mM stock solution in DMSO) for 45 min. at 37°C for evaluating H_2O_2 generation. Dihydrorhodamine became oxidized to the cationic green fluorescent dye, rhodamine-123, which accumulated intracellularly due to electrically negative cytoplasmic and mitochondrial membrane potential. Fluorescent cells were quantified under a fluorescence microscope (Zeiss Axiostart 50) by counting a minimum of 300 total cells as follows: % fluorescent positive H_2O_2 cells (observed as completely green bright fluorescent cells) = 100 × (number of green fluorescent cells) / total number of cells (green fluorescent cells + non-fluorescent cells) compared to the untreated control. The experiments were performed in three independent settings. Parallel to $O_2\bullet^-$ and H_2O_2 evaluation, apoptotic cell percentage was established according to an AO/EB staining assay.

Qualitative analysis of mitochondrial membrane potential ($\Delta\Psi_m$). The peripheral blood lymphocytes were treated as described above; they were incubated for 15 min. at 37°C with cationic lipophilic $DiOC_6(3)$ (1 μM, final concentration) to evaluate $\Delta\Psi_m$. Fluorescent cells (reflecting high-polarized and low-polarized mitochondria) were quantified under a fluorescence microscope by counting a minimum of 300 total cells as follows: % $DiOC_6(3)$ positive fluorescent cells = 100 × (number of $DiOC_6(3)^{high/low}$ fluorescent cells) / total number of cells (non-fluorescent cells, reflecting depolarized mitochondria, plus $DiOC_6(3)^{high/low}$ fluorescent cells) compared to untreated cells (positive control). The experiments were performed in three independent settings.

Assessment of natural or synthetic antioxidant potential in lymphocytes exposed to rotenone. The peripheral blood lymphocytes were incubated with 250 μM rotenone and the other products of interest listed in table 3 for 24 hr. at 37/C. Treated peripheral blood lymphocytes were then evaluated for apoptotic morphology and $\Delta\Psi_m$ as described above.

Immunocytochemistry detection of NF-κB, p53 and c-Jun transcription factor proteins. The supplier's protocol (Santa Cruz Biotechnology Inc., Santa Cruz, CA, USA; goat ABC staining System: cat # sc-2023) was followed for the immunocytochemistry using primary goat polyclonal antibodies NF-κB p65 (C-20)-G (Santa Cruz

Biotechnology cat#sc-372-G), p53 (FL-393) (Santa Cruz Biotechnology cat #sc-6243-G) and p-(Ser 73)-c-Jun (Santa Cruz Biotechnology cat #sc-7981). The cells were plated on poly-L-lysine-coated cover slips after treatment and fixed in 4% methanol in 0.1 M phosphate buffer, pH 7.4 for 25 min. and then washed with phosphate-buffered saline. The slides were exposed to a 1% hydrogen peroxide solution in phosphate-buffered saline for 10 min. After several washes, cells were permeabilized with Triton X-100 solution in phosphate-buffered saline for 5 min. The cells were incubated with primary antibodies (10 μg/ml) for 2 hr. at room temperature and subsequently incubated with biotinylated antibody at room temperature for 1 hr. The specimens were stained with an ABC enzyme kit; they were cover-slipped with cover glasses after staining.

Photomicrography. The light microscopy or fluorescent photomicrographs shown in figs 1 and 4 were taken using a Zeiss (Axiostart 50) microscope equipped with a Canon PowerShot G5 digital camera.

Results

Rotenone induced apoptosis in lymphocytes through anion superoxide radical ($O_2\bullet^-$)/H_2O_2 generation and mitochondrial damage: the protective effect of IGF-1.

It is known that rotenone promotes endogenous generation of reactive oxygen species (ROS) in different dopaminergic neural cell lines. Similarly, peripheral blood lymphocyte cells treated with rotenone generated both $O_2\bullet^-$, as determined by nitroblue tetrazolium reduction into formazan, and H_2O_2 as detected by the oxidation of dihydrorhodamine into rhodamine-123 (R-123) (figs 1A and B). Whilst high rotenone concentrations (e.g. 100–250 μM) produced 18–43% formazan and 21–45% R-123, low concentrations (e.g. 1–10 μM) yielded formazan and R-123 percentages comparable to those for untreated cells (fig. 2). Rotenone's effect on mitochondrial membrane potential (fig. 1C) and its relationship with apoptosis was thus investigated. It was found that peripheral blood lymphocytes exposed to either 100 or 250 μM rotenone induced moderate mitochondrial depolarization, i.e. 18% and 36% $D_iOC_6(3)$ negative cells, respectively. By contrast, no effect on mitochondrial potential was observed when peripheral blood lymphocytes were incubated with either 1 or 10 μM rotenone, i.e. almost 100% $D_iOC_6(3)$ positive cells compared to untreated cells (fig. 2). Parallel examination of peripheral blood lymphocytes exposed to increasing rotenone concentrations (1–250 μM) induced the typical morphological characteristics of apoptosis, such as chromatin condensation (i.e. highly condensed nuclei) and chromatin fragmentation into ring-, horse-shoe- and moon-like shapes in peripheral blood lymphocyte cells, as analysed by conventional AO/EB staining technique (fig. 1D). Fig. 2 shows that while 100 μM and 250 μM rotenone induced around 18–34% apoptosis, respectively, 1 and 10 μM rotenone provoked apoptosis comparable to untreated cells; 250 μM rotenone was thus selected for further experiments.

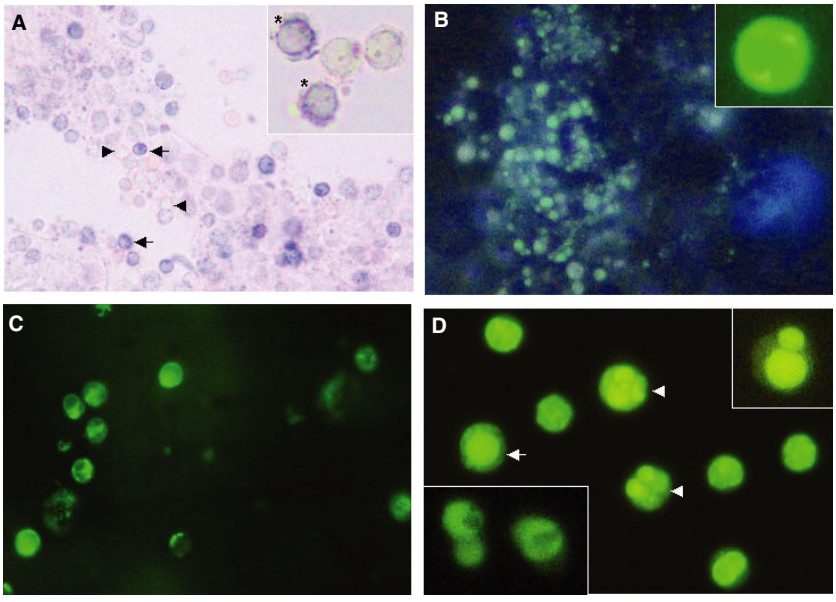

Fig. 1. Rotenone induced $O_2\bullet^-/H_2O_2$ generation and apoptosis in lymphocytes. Representative light photomicrography showing positive nitroblue tetrazolium stained blue–purple precipitate cells (i.e. formazan, *arrows*) as positive $O_2\bullet^-$ generation and nitroblue tetrazolium negative stained cells (i.e. translucent cells, *arrowheads*) from cells treated with 250 μM rotenone for 6 hr. *Inset:* Magnification of two positive nitroblue tetrazolium cells (*asterisk*) showing cytoplasmic blue–purple precipitate whereas negative nitroblue tetrazolium cells are cytoplasmic translucent; (B) Fluorescent photomicrography (ex. 365/12 nm, em. 397 nm) illustrating positive R-123 fluorescent stained cells as positive H_2O_2 production from peripheral blood lymphocytes treated with 250 μM rotenone for 6 hr. *Inset*: Magnification of a typical positive R-123 cell showing intense green fluorescence (ex. 450–490 nm, em. 515 nm); (C) Representative fluorescent photomicrography (ex. 450–490 nm, em. 515 nm) illustrates positive green fluorescent stained cells as $D_iOC_6(3)$ high-polarized and low-polarized mitochondria from untreated peripheral blood lymphocytes for 24 hr. The picture represents one out of three independent observations; (D) Representative fluorescent photomicrography (ex. 450–490 nm, em. 515 nm) showing typical nuclear apoptotic morphology such as highly condensed chromatin (*arrow*) and nuclear fragmentation (*arrowheads*) from lymphocytes treated with 250 μM rotenone for 24 hr. Magnification (A–C) 400×. Magnification (D) 600×. Magnification insets 800×.

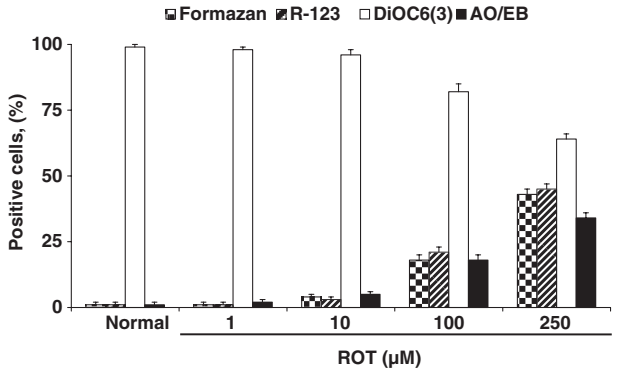

Fig. 2. Rotenone produced reactive oxygen species, mitochondrial damage and apoptosis in lymphocytes. Lymphocytes were incubated with increasing concentrations of rotenone (ROT) for 24 hr. $O_2\bullet^-$, H_2O_2, mitochondrial potential and apoptosis were evaluated as described in *Materials and Methods*. The percentage of positive formazan, R-123, $D_iOC_6(3)$ high-polarized and low-polarized mitochondria and AO/EB stained cells are expressed as mean percentage ±S.D. from three independent experiments.

This led to evaluating whether IGF-1 was able to protect lymphocytes against rotenone toxicity and determined its impact on ROS, mitochondrial potential, and apoptotic morphology. Fig. 3 shows that rotenone (250 μM) alone (vehicle) or co-incubated with increasing IGF-1 concentrations (1–250 nM) induced almost constant generation of $O_2\bullet^-$ and H_2O_2 (e. g. 35–43% formazan positive cells and 34–45% R-123 positive cells, respectively). Noticeably, peripheral blood lymphocyte cells treated with high IGF-1 concentrations (100–250 nM) were protected from the noxious effect of 250 μM rotenone compared to low IGF-1 concentrations (1–10 nM) and to peripheral blood lymphocyte cells treated with rotenone. The IGF-1 protective effect also correlated well with mitochondrial functionality (e.g. 91–96% $D_iOC_6(3)$ positive cells); 250 nM IGF-1 was thus used as protective agent for further assays.

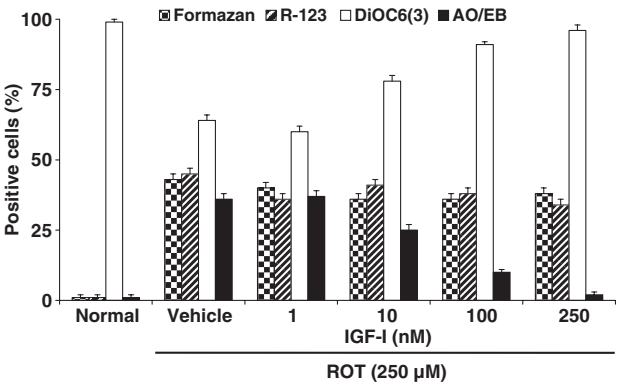

Fig. 3. IGF-1 protected lymphocytes against rotenone-induced apoptosis in lymphocytes, independently of reactive oxygen species. Lymphocytes were incubated alone (normal), rotenone (ROT) (250 μM) or with rotenone (250 μM) in a combination of increasing IGF-1 concentrations for 24 hr. $O_2\bullet^-$, H_2O_2, and apoptosis were evaluated as described in *Materials and Methods*. The percentage of positive formazan, R-123, $D_iOC_6(3)$ high-polarized and low-polarized mitochondria and AO/EB stained cells are expressed as mean percentage ±S.D. from three independent experiments.

IGF-1 protected lymphocytes against rotenone through PI-3K/NF-κB activation and p53 and caspase-3 inhibition.

Cells were exposed to rotenone (250 μM) and IGF-1 alone (250 nM) or in the presence of LY294002 (5 μM, a specific PI-3 kinase pathway inhibitor) and PD98059 (5 μM, a specific MEK-1 pathway inhibitor) chemical compounds to investigate the mechanism by which IGF-1 protects lymphocytes from rotenone-induced apoptosis. Table 1 shows that LY294002 blocked IGF-1's anti-apoptotic effect against rotenone toxicity to almost control value (i.e. rotenone alone: 34% AO/EB technique); however, PD98059 was unsuccessful on inhibiting IGF-1 action against rotenone-induced apoptosis (e.g. 4% AO/EB staining). Consequently, LY294002 blocked IGF-1's protective effect on maintaining $\Delta\Psi_m$ in the presence of rotenone. By contrast, IGF-1 protected and maintained mitochondrial potential to control values (i.e. 4% AO/EB staining, 1% $D_iOC_6(3)$ staining) when co-incubated with PD98059 and rotenone. Of note, LY294002 and PD98059 were innocuous to peripheral blood lymphocytes when incubated alone or with rotenone.

Lymphocytes were incubated for 1 hr. with PDTC (10 nM, specific NF-κB inhibitor), PFT (50 nM, specific p53 inhibitor), SP600125 (1 μM, specific c-Jun N-terminal protein kinase inhibitor), DEVD (10 μM, specific caspase-3 inhibitor) inhibitors to investigate whether rotenone's toxic effect was related to transcription factor and caspase-3 activation. Lymphocytes were then exposed to (250 μM) rotenone for 24 hr. Table 1 shows that specific pharmacological inhibitors moderately reduced rotenone-induced apoptosis in peripheral blood lymphocytes by 56–76%. Immunocytochemical assessment also confirmed NF-κB, p53 and c-Jun participation in rotenone-induced toxicity. Fig. 4 shows that IGF-1 induced NF-κB activation and translocation to the nucleus (fig. 4D, DAB-positive nuclei), whereas rotenone-induced NF-κB, p53 and c-Jun activation and translocation (fig. 4G–I), compared to untreated peripheral blood lymphocyte cells (fig. 4A–C). It should be noted that NF-κB and c-Jun activation and nuclei translocation was observed when lymphocytes were incubated with IGF-1 and rotenone (figs 4J and L).

IGF-1 and pharmacological compounds rescued lymphocytes against rotenone-induced apoptosis.

Lymphocytes were exposed to 250 μM rotenone for 1, 3, 6, 12 and 24 hr. to establish the particular time at which rotenone induced apoptosis and to establish its relationship with ROS generation. Fig. 5 shows that rotenone evoked a progressively increasing occurrence of apoptosis and $O_2\bullet^-$ production in peripheral blood lymphocytes at each time interval. Since rotenone exposure yielded around 15% apoptosis and ROS at 6 hr. (fig. 5) compared to 24 hr. for rotenone exposure (i.e. 34% apoptosis), this time interval was set up to test whether IGF-1, PDTC, PFT, SP600125 and DEVD were able to rescue lymphocytes against rotenone

Table 1.

The effect of IGF-1, and PI3K, MEK-1, NF-κB, c-Jun, p53 and caspase-3 inhibitors on lymphocytes after being exposed to rotenone.

Treatment	AO/EB (%)	$DiOC_6(3)^{high/low}$ (%)
Untreated	1 ± 0	99 ± 0
IGF-1 (250 nM)	0	100
ROT (250 μM)	34 ± 2	64 ± 3
IGF-1 (250 nM) + ROT (250 μM)	3 ± 1	96 ± 2
LY294002 (5 μM)	1 ± 0	99 ± 0
LY294002 (5 μM) + IGF-1 (250 nM)	0	100
LY294002 (5 μM) + ROT (250 μM)	36 ± 2	64 ± 2
LY294002 (5 μM) + IGF-1 (250 nM) + ROT (250 μM)	35 ± 2	63 ± 3
PD98059 (5 μM)	1 ± 0	99 ± 0
PD98059 (5 μM) + IGF-1 (250 nM)	0	100
PD98059 (5 μM) + ROT (250 μM)	36 ± 3	65 ± 2
PD98059 (5 μM) + IGF-1 (250 nM) + ROT (250 μM)	4 ± 1	96 ± 2
PDTC (10 nM)	1 ± 0	99 ± 0
PDTC (10 nM) + IGF-1 (250 nM)	0	100
PDTC (10 nM) + ROT (250 μM)	15 ± 2	86 ± 3
PDTC (10 nM) + IGF-1 (250 nM) + ROT (250 μM)	1 ± 1	98 ± 2
PFT (50 nM)	1 ± 0	99 ± 0
PFT (50 nM) + IGF-1 (250 nM)	0	100
PFT (50 nM) + ROT (250 μM)	12 ± 2	90 ± 3
PFT (50 nM) + IGF-1(250 nM) + ROT (250 μM)	1 ± 1	98 ± 2
SP600125 (1 μM)	0	100
SP600125 (1 μM) + IGF-1 (250 nM)	0	100
SP600125 (1 μM) + ROT (250 μM)	8 ± 2	88 ± 2
SP600125 (1 μM) + IGF-1(250 nM) + ROT (250 μM)	3 ± 1	96 ± 2
DEVD (10 μM)	0	100
DEVD (10 μM) + IGF-1 (250 nM)	0	100
DEVD (10 μM) + ROT (250 μM)	10 ± 2	89 ± 2
DEVD (10 μM) + IGF-1(250 nM) + ROT (250 μM)	1 ± 1	98 ± 2

Cells were left untreated or treated with specific PI3K, MEK-1, NF-κB, c-Jun, p53 and caspase-3 inhibitors, such as LY294002 (5 μM), PD98059 (5 μM), ammonium pyrrolidinedithiocarbamate (PDTC, 10 nM), SP600125 (1 μM), pifithrin-α (PFT, 50 nM), and DEVD (10 μM) alone or in the presence of rotenone (250 μM) for 24 hr. After this time, mitochondrial membrane potential and nuclear morphological changes resulting from PI3K, NF-κB-, p53 and caspase-3 activation were evaluated using $D_iOC_6(3)$ and AO/EB staining, as described in *Materials and Methods*. High-polarized and low-polarized mitochondria (green fluorescent $D_iOc_6(3))^{high/low}$ positive cells) and apoptosis percentage is expressed as mean percentage (%) ±S.D. from two independent experiments.

toxicity. Lymphocytes were thus pre-exposed to rotenone for 6 hr.; cells were then incubated in the absence (medium alone) or presence of IGF-1 (250 nM) and selected inhibitors for an additional 24 hr. Table 2 shows that IGF-1 and inhibitors were effective in rescuing cells from rotenone noxious effects.

Lymphocytes were protected against rotenone-induced cell death by glucose and antioxidants.

It was also investigated whether glucose and antioxidants protected lymphocytes against rotenone. Table 3 shows that glucose (55.5 mM), cannabinoids (100 nM JWH-015 and CP55,940) and Vitamin E (0.5 mM) were all fully efficient in protecting cells from rotenone toxicity.

Discussion

This work reports, for the first time, that IGF-1 was effective in suppressing rotenone-induced apoptosis in lymphocytes. The toxic effect of rotenone (a specific mitochondrial inhibitor complex-I) was initially investigated in these cells as the rotenone-induced cell death mechanism is still controversial. In fact, lymphocytes displayed typical apoptotic morphology features, such as chromatin condensation and/or nuclei fragmentation in a concentration-dependent fashion as early as 6 hr. rotenone treatment. Marella *et al.* [17] found that undifferentiated PC12 incubated with increasing rotenone concentrations (50 nM up to 1 μM) for 4 days induced steadily decreasing cell viability, having 75% maximal trypan blue positive cell value. This observation and our results thus suggest that rotenone provokes time- and dose-dependent apoptosis. Since rotenone is a lipophilic compound and no specific transporter for rotenone has been identified to date, rotenone might easily be taken up by cells. Indeed, rotenone not only targets mouse and rat primary mesencephalic dopaminergic cells [11,37,38], organotypic *substantia nigra* culture dopaminergic neurons [39], undifferentiated SK-N-MC [17] and SH-SY5Y neuroblastoma cells [9] and undifferentiated PC12 cells [17] but also destroys HL-60 (the human promyelocytic leukaemia cell line) [13,14] and human peripheral blood lymphocytes (this work). This information implies that rotenone behaves as a non-specific cell type toxin which is able to interact with and selectively impaired mitochondrial complex-I function; however, the mechanism by which

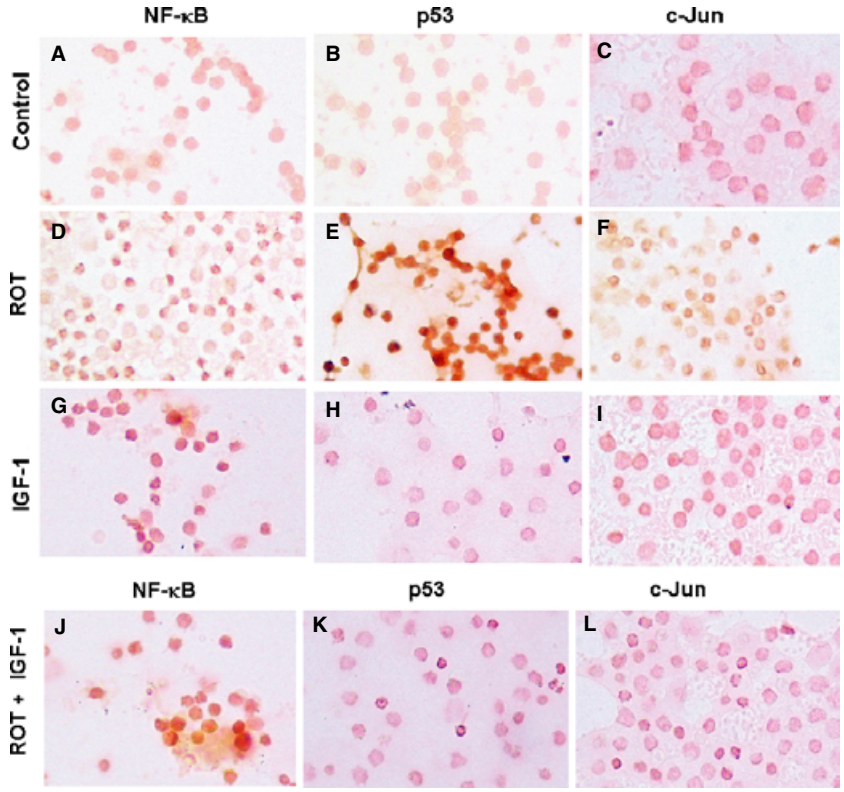

Fig. 4. Rotenone (ROT) induced simultaneous NF-κB, p53 and c-Jun transcription factor activation in lymphocytes. Peripheral blood lymphocytes cells were left untreated (A–C), exposed to 250 μM rotenone (D–F), 250 nM IGF-1 (G–I), and to 250 nM IGF-1 + 250 μM rotenone (J–L) for 24 hr. After the incubation period, cells were stained with anti-NF-κB-p65 (A,D,G,J), anti-p53 (B,E,H,K) and anti-c-Jun (C,F,I,L) antibodies according to the procedure described in *Materials and Methods*. Notice that NF-κB, p53 and c-Jun positive-nuclei (dark brown) reflect their nuclear translocation/activation. Magnification 400× (A–L).

rotenone provokes apoptosis still remains controversial. Our data have suggested that rotenone induced apoptosis in lymphocytes via an oxidative stress mechanism. This conclusion was based on the following observations. First, it was confirmed that rotenone generated $O_2\bullet^-/H_2O_2$ [13,14] and that their production was associated with decreased mitochondrial membrane potential and morphological apoptotic nuclei. Second, antioxidant compounds such as JWH-015, CP55940, Vit E and NAC reduced apoptosis and restored mitochondrial potential to control values. In agreement with these findings, Li *et al.* [14] found that (1 μM) rotenone-induced apoptosis in HL-60 cells was inhibited by treatment with the antioxidant (10–15 mM) glutathione, NAC and Vitamin C. Third, lymphocytes co-incubated with glucose were able to maintain mitochondrial potential functionality and nuclear morphology against rotenone toxicity to control values (i.e. 100% $D_iOC_6(3)$ fluorescent staining and <1% AO/EB nuclear staining). Accordingly, it has been reported that both pyruvate or sodium pyruvate (a natural metabolic intermediate scavenger of reactive oxygen species) inhibited $\Delta\Psi m$ collapse and apoptosis from H_2O_2-induced oxidative stress in the human neuroblastoma SK-N-SH [40] and SK-N-MC cell lines [41]. These data agreed with the notion that mitochondria de-energize and depolarize after rotenone/ROS exposure, thereby leading to apoptotic cell morphology. Indeed, adding (100 μM) H_2O_2 to lymphocytes resulted in impairing mitochondrial membrane potential and inducing apoptosis [42].

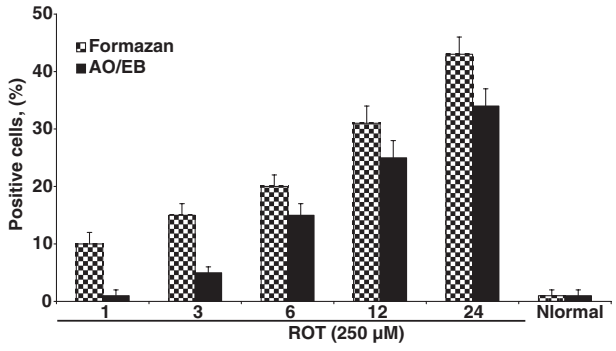

Fig. 5. Rotenone (ROT) induced ROS and apoptotic nuclei in a time-dependent fashion. Lymphocytes were either left untreated (normal) or treated with rotenone (250 μM) for 1, 3, 6, 12 and 24 hr. The percentage of positive formazan and AO/EB stained cells after each interval are expressed as a mean percentage ±S.D. from three independent experiments.

The present work has shown, for first time, that transcription factor NF-κB and p53 activation were involved in rotenone death signalling, as assessed by immunohistochemical staining with primary antibodies against those factors and

Table 2.

IGF-1 and pharmacological compounds rescued lymphocytes from ROT-induced apoptosis.

Treatment	AO/EB (%)	$DiOC_6(3)^{high/low}$ (%)
Untreated	1 ± 0	99 ± 0
IGF-1 (250 nM)	0	100
ROT (250 μM)[1]	54 ± 2	55 ± 3
IGF-1 (250 nM) + ROT (250 μM)	6 ± 2	90 ± 3
LY294002 (5 μM)	1 ± 0	99 ± 0
LY294002 (5 μM) + ROT (250 μM)	50 ± 2	53 ± 3
PD98059 (5 μM)	1 ± 0	99 ± 0
PD98059 (5 μM) + ROT (250 μM)	47 ± 3	50 ± 3
PDTC (10 nM)	1 ± 0	99 ± 0
PDTC (10 nM) + ROT (250 μM)	7 ± 2	90 ± 3
PFT (50 nM)	1 ± 0	99 ± 0
PFT (50 nM) + ROT (250 μM)	8 ± 2	92 ± 3
SP600125 (1 μM)	1 ± 0	99 ± 0
SP600125 (1 μM) + ROT (250 μM)	4 ± 1	98 ± 2
DEVD (10 μM)	1 ± 0	99 ± 0
DEVD (10 μM) + ROT (250 μM)	1 ± 1	98 ± 2

Lymphocytes were pre-exposed to rotenone for 6 hr. After this time, cells were incubated in the absence (medium alone) or presence of IGF-1 (250 nM) and selected inhibitors for an additional 24 hr. High-polarized and low-polarized mitochondria (green fluorescent $D_iOc_6(3))^{high/low}$ positive cells) and apoptosis percentage is expressed as mean percentage (%) ±S.D. from three independent experiments.
[1]Rotenone was incubated for 30 hr.

pharmacological inhibition using PDTC and PFT-α. As for rotenone, other well-characterized redox cycling neurotoxins (e.g. 6-hydroxydopamine [6-OHDA]) have been shown to activate transcription factors both *in vitro* [42–44] and *in vivo* [45]. Moreover, blocking NF-κB nuclear translocation and p53 induction reduced nigral dopaminergic degeneration [45,46]. Taken together, this information and our results suggested that NF-κB and p53 were decisive factors in lymphocyte death [47–51]. Pharmacological blockage of NF-κB might thus offer an interesting neuroprotective strategy against oxidative stress [52].

Table 3.

Glucose and antioxidant compounds protected against rotenone toxicity.

Treatment/assay	AO/EB (%)	$DiOC_6(3)^{high/low}$ (%)
Untreated	1 ± 0	99 ± 0
ROT (250 μM)	34 ± 2	64 ± 3
GLU (55.5 mM)	1 ± 1	98 ± 2
GLU (55.5 mM) + ROT (250 μM)	5 ± 2	93 ± 2
JWH-015 (100 nM)	1 ± 0	99 ± 0
JWH-015 (100 nM) + ROT (250 μM)	2 ± 1	98 ± 2
CP55,940 (100 nM)	1 ± 0	99 ± 0
CP55,940 (100 nM) + ROT (250 μM)	4 ± 2	97 ± 2
Vit E (0.5 mM)	1 ± 0	99 ± 0
Vit E (0.5 mM) + ROT (250 μM)	3 ± 1	98 ± 2
NAC (1 mM)	1 ± 0	99 ± 0
NAC (1 mM) + ROT (250 μM)	2 ± 1	98 ± 2

Lymphocyte cells were incubated with rotenone (250 μM) in the absence or presence of glucose (55.5 mM), JWH-O15 (100 nM), CP55,940 (100 nM), Vit E (0.5 mM) and NAC (1 mM) for 24 hr. After this time, mitochondrial membrane potential and nuclear morphological changes were evaluated using $D_iOC_6(3)$ and AO/EB staining, as described in *Materials and Methods*. High-polarized and low-polarized mitochondria (green fluorescent $D_iOc_6(3))^{high/low}$ positive cells) and apoptosis percentage is expressed as mean percentage (%) ±S.D. from three independent experiments.

Our data indicated that the SP600125 c-Jun N-terminal protein kinase inhibitor had protective effects against rotenone toxicity. This result agreed with the notion that c-Jun N-terminal protein kinase and c-Jun activation is required for rotenone-induced apoptosis in lymphocytes and dopaminergic neurons [15]. Furthermore, this is the first report in an *in vitro* study in which simultaneous NF-κB and c-Jun activation in rotenone/(H_2O_2)-induced apoptosis signalling has been demonstrated. These observations imply 'cross-talk' between NF-κB and c-Jun N-terminal protein kinase signalling pathways [53]. These sets of data are in agreement with the notion that NF-κB and c-Jun N-terminal protein kinase activation are critical transcription factors contributing to oxidative stress-mediated cell death in lymphocytes via an NF-κB/c-Jun N-terminal protein kinase-dependent p53-signaling pathway [54,55].

Mitochondria are organelles which play a crucial role in apoptosis (for a review, see ref [56]). Indeed, mitochondrial control of apoptosis has been described at ATP production, mitochondrial membrane potential and mitochondrial membrane permeability level regarding the release of certain apoptogenic factors from the inter-membrane space into the cytosol, in turn activating executor proteins such as caspase-3. In agreement with others, it was found that rotenone induced change in mitochondria membrane potential [13,14], caspase-3 activation [11–14] and nuclei fragmentation. The above observations thus comply with the idea that rotenone-induced apoptosis in lymphocytes is mediated by H_2O_2 mitochondrial membrane potential disruption, and caspase-3 activation. Although the probable participation of other pro-apoptotic proteins in rotenone-provoked cell death cannot be disregarded [17], the results presented here support the notion that caspase-3 plays a crucial role in dismantling lymphocyte cells.

Part of the present investigation was to identify the specific molecular mechanism responsible for IGF-1 protection of lymphocytes against rotenone. It has been demonstrated that IGF-1 effectively induced concentration-dependent lymphocyte protection against rotenone. Moreover, IGF-1 (250 nM) almost completely abolished the rotenone-induced toxic effect. Interestingly, such protective effect was independent of rotenone-generated ROS but IGF-I's cytoprotective effect was closely related to mitochondrial protection [57]. These results were thus in line with the notion that the IGF-1 protective mechanism is dependent on IGF-1 signalization and mitochondrial membrane potential maintenance rather than antioxidant reactions. Specific inhibitor LY294002, but not PD98059, was effective in blocking the IGF-1 protective effect. Taken together, these observations thus suggest that PI-3K/Akt rather than the MEK signalling pathway is involved in IGF-1 cytoprotection against oxidative

stress-induced apoptosis, not only in non-neuronal cells [20,58] but also in neuronal cells [59]. In the same vein, it was found, for the first time, that IGF-1 simultaneously induced p53 down-expression and NF-κB over-expression in lymphocytes on being exposed to rotenone. Consequently, neither appreciable mitochondrial depolarization nor nuclei damage was detected. These findings are thus consistent with the idea that IGF-1 can block cell death by modulating apoptotic machinery at p53 level. Moreover, antioxidant and IGF-1 were able to rescue lymphocytes pre-incubated with rotenone by reducing rotenone-induced ROS. These data suggest that antioxidants and IGF-1 can reverse fatal effects on cells. Our findings have thus revealed that p53 but not NF-κB is the critical transcription factor which may possibly balance pro-death cell decision under noxious stimuli. These data may contribute to understanding the role played by oxidative stress stimuli and IGF-1's molecular counteraction.

Acknowledgements

This work was supported by Colciencias grants #1115-343-19119 awarded to M Jimenez-Del-Rio. We would like to thank C Aguirre-Acevedo from the University of Antioquia, Neuroscience Research Group, for statistical analysis. I.C.A-G is a recipient of a doctoral scholarship from Colciencias, contract # 8790-046-07 and is enrolled in the Biomedical Science Program-UdeA.

References

1 Schapira AH. Mitochondria in the aetiology and pathogenesis of Parkinson's disease. Lancet Neurol 2008;**7**:97–109.
2 Belin AC, Westerlund M. Parkinson's disease: a genetic perspective. FEBS J 2008;**275**:1377–83.
3 Landrigan PJ, Sonawane B, Butler RN, Trasande L, Callan R, Droller D. Early environmental origins of neurodegenerative disease in later life. Environ Health Perspect 2005;**113**:1230–3.
4 Hancock DB, Martin ER, Mayhew GM, Stajich JM, Jewett R, Stacy MA *et al.* Pesticide exposure and risk of Parkinson's disease: a family-based case-control study. BMC Neurol 2008;**8**:6.
5 Bové J, Prou D, Perier C, Przedborski S. Toxin-induced models of Parkinson's disease. NeuroRx 2005;**2**:484–894.
6 Sherer TB, Richardson JR, Testa CM, Seo BB, Panov AV, Yagi T *et al.* Mechanism of toxicity of pesticides acting at complex I: relevance to environmental etiologies of Parkinson's disease. J Neurochem 2007;**100**:1469–79.
7 Lenaz G, Fato R, Genova ML, Bergamini C, Bianchi C, Biondi A. Mitochondrial Complex I: structural and functional aspects. Biochim Biophys Acta 2006;**1757**:1406–20.
8 Sherer TB, Betarbet R, Testa CM, Seo BB, Richardson JR, Kim JH *et al.* Mechanism of toxicity in rotenone models of Parkinson's disease. J Neurosci 2003;**23**:10756–64.
9 Watabe M, Nakaki T. ATP depletion does not account for apoptosis induced by inhibition of mitochondrial electron transport chain in human dopaminergic cells. Neuropharmacology 2007;**52**:536–41.
10 Kweon GR, Marks JD, Krencik R, Leung EH, Schumacker PT, Hyland K *et al.* Distinct mechanisms of neurodegeneration induced by chronic complex I inhibition in dopaminergic and non-dopaminergic cells. J Biol Chem 2004;**279**:51783–92.
11 Moon Y, Lee KH, Park JH, Geum D, Kim K. Mitochondrial membrane depolarization and the selective death of dopaminergic neurons by rotenone: protective effect of coenzyme Q10. J Neurochem 2005;**93**:1199–208.
12 Ahmadi FA, Linseman DA, Grammatopoulos TN, Jones SM, Bouchard RJ, Freed CR *et al.* The pesticide rotenone induces caspase-3-mediated apoptosis in ventral mesencephalic dopaminergic neurons. J Neurochem 2003;**87**:914–21.
13 Tada-Oikawa S, Hiraku Y, Kawanishi M, Kawanishi S. Mechanism for generation of hydrogen peroxide and change of mitochondrial membrane potential during rotenone-induced apoptosis. Life Sci 2003;**73**:3277–88.
14 Li N, Ragheb K, Lawler G, Sturgis J, Rajwa B, Melendez JA *et al.* Mitochondrial complex I inhibitor rotenone induces apoptosis through enhancing mitochondrial reactive oxygen species production. J Biol Chem 2003;**278**:8516–25.
15 Klintworth H, Newhouse K, Li T, Choi WS, Faigle R, Xia Z. Activation of c-Jun N-terminal protein kinase is a common mechanism underlying paraquat- and rotenone-induced dopaminergic cell apoptosis. Toxicol Sci 2007;**97**:149–62.
16 Ramachandiran S, Hansen JM, Jones DP, Richardson JR, Miller GW. Divergent mechanisms of paraquat, MPP+, and rotenone toxicity: oxidation of thioredoxin and caspase-3 activation. Toxicol Sci 2007;**95**:163–711.
17 Marella M, Boo-Seo B, Matsuno-Yagi A, Yagi T. Mechanism of cell death caused by complex I defects in a rat dopaminergic cell line. J Biol Chem 2007;**282**:24146–56.
18 Hartley A, Stone JM, Heron C, Cooper JM, Schapira AH. Complex I inhibitors induce dose-dependent apoptosis in PC12 cells: relevance to Parkinson's disease. J Neurochem 1994;**63**:1987–90.
19 Kooijman R. Regulation of apoptosis by insulin-like growth factor (IGF)-I. Cytokine Growth Factor Rev 2006;**17**:305–23.
20 Jimenez-Del-Rio M, Velez-Pardo C. Insulin-like growth factor-1 prevents $A\beta_{[25-35]}/(H_2O_2)$-induced apoptosis in lymphocytes by reciprocal NF-κB activation and p53 inhibition via PI3K-dependent pathway. Growth Factors 2006;**24**:67–78.
21 Kurmasheva RT, Houghton PJ. IGF-1 mediated survival pathways in normal and malignant cells. Biochim Biophys Acta 2006;**1766**:1–22.
22 O'Neill MJ, Messenger MJ, Lakics V, Murray TK, Karran EH, Szekeres PG *et al.* Neuroreplacement, growth factor, and small molecule neurotrophic approaches for treating Parkinson's disease. Int Rev Neurobiol 2007;**77**:179–217.
23 Cude K, Wang Y, Choi HJ, Hsuan SL, Zhang H, Wang CY *et al.* Regulation of the G2-M cell cycle progression by the ERK5-NFkappaB signaling pathway. J Cell Biol 2007;**177**:253–64.
24 Marino F, Cosentino M, Bombelli R, Ferrari M, Lecchini S, Frigo G. Endogenous catecholamine synthesis, metabolism, storage, and uptake in human peripheral blood mononuclear cells. Exp Hematol 1999;**27**:489–95.
25 Amenta F, Bronzetti E, Cantalamessa F, El-Assouad D, Felici L, Ricci A *et al.* Identification of dopamine plasma membrane and vesicular transporters in human peripheral blood lymphocytes. J Neuroimmunol 2001;**117**:133–42.
26 Ricci A, Amenta F. Dopamine D5 receptors in human peripheral blood lymphocytes: a radioligand binding study. J Neuroimmunol 1994;**53**:1–7.
27 Ricci A, Veglio F, Amenta F. Radioligand binding characterization of putative dopamine D3 receptor in human peripheral blood lymphocytes with [3H] 7-OH-DPAT. J Neuroimmunol 1995;**58**:139–44.
28 Ricci A, Bronzetti E, Felici L, Tayebati SK, Amenta F. Dopamine D4 receptor in human peripheral blood lymphocytes: a radioligand binding assay study. Neurosci Lett 1997;**229**:130–4.
29 Amenta F, Bronzetti E, Felici L, Ricci A, Tayebati SK. Dopamine D2-like receptors on human peripheral blood lymphocytes: a

radioligand binding assay and immunocytochemical study. J Auton Pharmacol 1999;**19**:151–9.
30 McKenna F, McLaughlin PJ, Lewis BJ, Sibbring GC, Cummerson JA, Bowen-Jones D *et al.* Dopamine receptor expression on human T- and B-lymphocytes, monocytes, neutrophils, eosinophils and NK cells: a flow cytometric study. J Neuroimmunol 2002;**132**:34–40.
31 Kerr JFR, Gobe GC, Winterford CM, Harmon BV. Anatomical methods in cell death. In: Schwartz LM, Osborne BA (eds). Methods in Cell Death. Academic Press, London, 1995;1–27.
32 Kalinichenko SG, Matveeva NY. Morphological characteristics of apoptosis and its significance in neurogenesis. Neurosci Behav Physiol 2008;**38**:333–44.
33 Tapson VF, Boni-Schnetzler M, Pilch PF, Center DM, Berman JS. Structural and functional characterization of the human T lymphocyte receptor for insulin-like growth factor I in vitro. J Clin Invest 1988;**82**:950–7.
34 Kooijman R, Willems M, Rijkers GT, Brinkman A, van Buul-Offers SC, Heijnen CJ *et al.* Effects of insulin-like growth factors and growth hormone on the in vitro proliferation of T lymphocytes. J Neuroimmunol 1992;**38**:95–104.
35 Melinn M, McLaughlin H. Nitroblue tetrazolium reduction in lymphocytes. J Leukoc Biol 1987;**41**:325–9.
36 Rothe G, Valet G. Flow cytometric assays of oxidative burst activity phagocytes. Methods Enzymol 1994;**233**:539–48.
37 Radad K, Rausch WD, Gille G. Rotenone induces cell death in primary dopaminergic culture by increasing ROS production and inhibiting mitochondrial respiration. Neurochem Int 2006;**49**:379–86.
38 Radad K, Gille G, Rausch WD. Dopaminergic neurons are preferentially sensitive to long-term rotenone toxicity in primary cell culture. Toxicol In Vitro 2008;**22**:68–74.
39 Testa CM, Sherer TB, Greenamyre JT. Rotenone induces oxidative stress and dopaminergic neuron damage in organotypic substantia nigra cultures. Brain Res Mol Brain Res 2005;**134**:109–18.
40 Wang X, Perez E, Liu R, Yan LJ, Mallet RT, Yang SH. Pyruvate protects mitochondria from oxidative stress in human neuroblastoma SK-N-SH cells. Brain Res 2007;**1132**:1–9.
41 Jagtap JC, Chandele A, Chopde BA, Shastry P. Sodium pyruvate protects against H(2)O(2) mediated apoptosis in human neuroblastoma cell line-SK-N-MC. J Chem Neuroanat 2003;**26**:109–18.
42 Jimenez-Del-Rio M, Velez-Pardo C. Paraquat induces apoptosis in human lymphocytes: protective and rescue effects of glucose, cannabinoids and insulin-growth factor-1. Growth Factors 2008;**26**:49–60.
43 Jimenez-Del-Rio M, Velez-Pardo C. Monoamine neurotoxin-induced apoptosis in lymphocytes by a common mechanism: involvement of hydrogen peroxide (H_2O_2), caspase-3, and nuclear factor kappa-B (NF-κB), p53, c-Jun transcription factor. Biochem Pharmacol 2002;**63**:677–88.
44 Velez-Pardo C, Garcia-Ospina G, Jimenez-Del-Rio M. Aβ[25-35] peptide and iron promote apoptosis in lymphocytes by a common oxidative mechanism: involvement of hydrogen peroxide (H_2O_2), caspase-3, NF-kappa B, p53 and c-Jun. NeuroToxicology 2002;**23**:351–65.
45 Liang ZQ, Li YL, Zhao XL, Han R, Wang XX, Wang Y *et al.* NF-kappaB contributes to 6-hydroxydopamine-induced apoptosis of nigral dopaminergic neurons through p53. Brain Res 2007;**1145**:190–203.
46 Li LY, Zhao XL, Fei XF, Gu ZL, Qin ZH, Liang ZQ. Bilobalide inhibits 6-OHDA-induced activation of NF-kappaB and loss of dopaminergic neurons in rat substantia nigra. Acta Pharmacol Sin 2008;**29**:539–47.
47 Aleyasin H, Cregan SP, Iyirhiaro G, O'Hare MJ, Callaghan SM, Slack RS *et al.* Nuclear factor-(kappa) B modulates the p53 response in neurons exposed to DNA damage. J Neurosci 2004;**24**:2963–73.
48 Ebadi M, Sharma SK, Wanpen S, Amornpan A. Coenzyme Q10 inhibits mitochondrial complex-1 down-regulation and nuclear factor-kappa B activation. J Cell Mol Med 2004;**8**:213–22.
49 Mogi M, Kondo T, Mizuno Y, Nagatsu T. p53 protein, interferon-gamma, and NF-kappaB levels are elevated in the parkinsonian brain. Neurosci Lett 2007;**414**:94–7.
50 Nijboer CH, Heijnen CJ, Groenendaal F, May MJ, van Bel F, Kavelaars A. Strong neuroprotection by inhibition of NF-kappaB after neonatal hypoxia-ischemia involves apoptotic mechanisms but is independent of cytokines. Stroke 2008;**39**:2129–37.
51 Wang X, Qin ZH, Shi H, Savitz SI, Qin AP, Jiang Y *et al.* Protective effect of Ginkgolids (A+B) is associated with inhibition of NIK/IKK/IkappaB/NF-kappaB signaling pathway in a rat model of permanent focal cerebral ischemia. Brain Res 2008;**1234**:8–15.
52 Pande V, Ramos MJ. NF-kappaB in human disease: current inhibitors and prospects for de novo structure based design of inhibitors. Curr Med Chem 2005;**12**:357–74.
53 Nakano H, Nakajima A, Sakon-Komazawa S, Piao JH, Xue X, Okumura K. Reactive oxygen species mediate crosstalk between NF-kappaB and JNK. Cell Death Differ 2006;**13**:730–7.
54 Hu MC, Qiu WR, Wang YP. JNK1, JNK2 and JNK3 are p53 N-terminal serine 34 kinases. Oncogene 1997;**15**:2277–87.
55 Oleinik NV, Krupenko NI, Krupenko SA. Cooperation between JNK1 and JNK2 in activation of p53 apoptotic pathway. Oncogene 2007;**26**:7222–30.
56 Kroemer G, Galluzzi L, Brenner C. Mitochondrial membrane permeabilization in cell death. Physiol Rev 2007;**87**:99–163.
57 Puche JE, García-Fernández M, Muntané J, Rioja J, González-Barón S, Castilla Cortazar I. Low doses of insulin-like growth factor-I induce mitochondrial protection in aging rats. Endocrinology 2008;**149**:2620–7.
58 Baregamian N, Song J, Jeschke MG, Evers BM, Chung DH. IGF-1 protects intestinal epithelial cells from oxidative stress-induced apoptosis. J Surg Res 2006;**136**:31–7.
59 Offen D, Shtaif B, Hadad D, Weizman A, Melamed E, Gil-Ad I. Protective effect of insulin-like-growth-factor-1 against dopamine-induced neurotoxicity in human and rodent neuronal cultures: possible implications for Parkinson's disease. Neurosci Lett 2001;**316**:129–32.

